Mass Transfer Controlled Corrosion of the Wall of Dual-Impeller Agitated Vessel

Yehia M. S. ElShazly

Abstract—In this research, the rate of mass transfer from the wall of a dual impeller agitated vessel was studied. The variable studied were the physical properties of the solution, the speed of rotation of the impellers and the length of the clearance between the two impellers. The dissolution of the copper wall in acidified dichromate solution was the technique applied to determine the values of the mass transfer coefficient. The results were correlated by the following dimensionless mass transfer equation:

$$Sh = 0.346\, Sc^{0.33} Re^{0.75} \left(\frac{c_2}{H}\right)^{0.185}$$

where c_2 is the distance between the two impellers and H is the liquid height in the vessel. The effect of addition of a drag reducing polymer and ceramic particles to the solution was also examined. The results showed a decrease of mass transfer with the addition of the polymer and an increase with the ceramic particles. The decrease accompanying the polymer addition was dependent on the agitation rate and the polymer concentration, while the increase accompanying the ceramic particles was dependent on the size, the amount, as well as the agitation rate.

Index Terms—Mass Transfer; Diffusion; Corrosion; Agitated Vessel; Dual Impeller; Drag Reducing Polymer; Suspended particles.

1 INTRODUCTION

AGITATED vessels are used to carry mixing, blending, suspending solids, intensifying mass and heat transfer, and increasing the homogeneity and the frequency of collision between reactant molecules in solutions [1], [2], [3]. Therefore they are always almost present in every chemical industry like the manufacture of chemicals, agrochemicals, pharmaceuticals, petrochemicals, paints, food, drinking water, wastewater treatment and minerals processing.

In recent years, multiple impellers agitated vessel have been finding ground in biochemical industrial processes where a shear sensitive micro-organisms are present [4]; For equivalent power input, impeller speeds will be lower and moderate shear values are generated in the vicinity of the impeller[5]. Moreover, the high height-to-diameter ratio of the vessel than the common value of the single impeller provides more compact design and increased gas hold up [5]. Regrettably, it is reported that the mixing time for dual impeller is higher than for a single impeller [6].

Various factors will affect the agitated vessel performance: the type of impeller, the clearance of the impeller from the bottom, the distance between the two impellers, the height-to-diameter ratio, the impeller diameter-to-tank diameter, and the baffles width [1], [3], [4].

Previous studies concluded that by varying the distance of the clearance between the two impellers, and the height of the bottom clearance, there would exist three different flow regimes [5], [7], [8], [9], [10], [11], [12], [13], [14], [15], [16], [17], [18]:

parallel (the impellers operate separately and independently of one another, and each impeller producing its own ring vortex and the impeller streams are almost horizontal and directed toward the vessel wall),

merging (the impeller streams follow an almost straight-line oriented toward one another and merge at a distance approximately midway between the impellers to form two large ring vortices,

diverging (the lower impeller stream follows a path toward and impinges upon the base of the vessel, while the flow from the upper impeller seems to be unaffected and directed horizontally to the wall).

These distinct flow regimes will have a great effect on the performance and applications of the vessel.

Furthermore, many additives can be present during the operation of the vessel; the use of drag reducing agents or suspended solid particles is not uncommon. Drag reducing polymers are used to reduce the frictional drag in turbulent flow and subsequently pressure loss with a resultant decrease in power consumption [19], [20], [21], [22], [23], [24], [25]. Their behavior was first reported by Toms [26] in 1948. Since then, different studies have documented their effects and proposed theories for their behavior: suppressing strong vorticity fluctuation neat the wall, quenching small scale eddies in the viscous sublayer, and damping penetration of low-speed fluid region into the high speed regions [27]. This was validated by the reported decrease of the associated rates of mass transfer [28], [29], [30], [31], [32] and heat transfer [33], [34]. However, the polymer action is known to function for a period of time before starting to degrade under the effect of

- *Yehia M.S. ElShazly is currently an Associate Professor at the Faculty of Engineering; Alexandria University; Egypt. PH:+201021618036; Email:yehia.elshazly@alexu.edu.eg*

turbulence and high shearing forces [35]. Also, many industrial processes such as dissolution / crystallization / leaching / adsorption / catalytic reactions [4],[36],[37] that require the presence of suspended solid particles in the solution of the vessel. These particles collide with the wall of the tank and erode the wall surface. Additionally, these particles will disturb the hydrodynamic and diffusion sublayers present near the wall. The synergic effect between the particle erosion and corrosion is widely reported [38], [39], [40], [41], [42], [43], [44], [45], [46], [47].

One of the major problems that affect the performance of the agitated vessels is the corrosion of its walls. Perforation of the tank wall would result in a shutdown, repair period and spillage control. It affects the designated service life of the tank. Moreover, corrosion products contaminate the solution: this can be considered a serious problem in processes involving bacteria [48], or food and pharmaceutical industries. Therefore, the study of the corrosion and determination of corrosion kinetics of agitated vessel is of prime importance. Corrosion of metals in aerated water is carried by the formation of galvanic cells at the surface of the metal. This process involves two simultaneous reactions: the anodic dissolution of metal, and the cathodic reduction of an oxidizing agent.

At the anodic sites, the metal oxidation and dissolution takes place (assumed here to be iron as steel is the most used material of construction for vessels):

Anode: $2\ Fe \rightarrow 2Fe^{++} + 4e^-$

At the cathodic sites, in neutral and alkaline medium, the oxygen reduction takes place [49]:

Cathode: $O_2+2H_2O+4e- \rightarrow 4\ OH^-$

The corrosion process under these conditions is found to be mass transfer controlled: the rate of corrosion is proportional to the rate of arrival of oxygen molecules from the bulk of solution to the cathodic sites, with no effect of the oxygen reduction rate on the overall rate [50],[51],[52].

Furthermore, the two reactions products then combine together to form the iron hydroxide as follows:

$2\ Fe^{++}+4OH- \rightarrow 2\ Fe(OH)_2$.

The $Fe(OH)_2$ deposit on the corroding surface oxidizes to form $Fe(OH)_3$ according to the reaction:

$2Fe+3/2\ O_2 + 3\ H_2O \rightarrow 2\ Fe(OH)_3$

The deposited $Fe(OH)_3$ film will form a barrier for the diffusion of the dissolved oxygen to the cathodic sites and supposedly reduces the rate of corrosion considerably. However, the fluid shear force results in the erosion and removal of the oxide film. Thus, the rate controlling will be only the oxygen transfer through the diffusion sublayer attached to the tank wall [50], [51], [52].

Under these conditions, the dissolved oxygen flux is given by:

$$N_{O_2} = k\left(C_{b_{O_2}} - C_{w_{O_2}}\right) \quad (1)$$

Where $C_{b_{O_2}}$ and $C_{b_{O_2}}$ are the concentrations of oxygen in the bulk of the solution and at the wall respectively; and k is the mass transfer coefficient. Under the conditions of diffusion controlled reaction, the oxygen reaching the wall goes directly into the reduction reaction, and thus its concentration is set to zero.

Accordingly, the equation for the flux of Fe can be calculated from the equation:

$$N_{Fe} = 2kC_{b_{O_2}} \quad (2)$$

The factor of 2 is to account that every molecule of oxygen reacts with 2 molecules of iron.

Eventually, the rate of corrosion of steel (CR), in mm/year, can be obtained from the mass transfer coefficient, k, according to the following equation [42]:

$$CR = \frac{2kC_{b_{O_2}} M.Wt._{Fe}}{\rho_{Fe}} \times 24 \times 60 \times 60 \times 365 \times 10^3 \quad (3)$$

Many techniques have been used to study the rate of solid/liquid mass transfer: the chemical reaction between the liquid and solid [28], [53], [54], [55], [56], [57], the dissolution of the sparingly soluble solid into liquid[58], [59], [60], [61], the electrochemical technique [62], [63], [64], [65], adsorption [66], [67], computational fluid dynamics [42], [68], [69], [70], and even has been followed with the scanning electron microscope [71].

In this research, the rate of mass transfer of the wall of a dual impeller agitated vessel is studied by an accelerated test: the diffusion and reaction of the hexavalent chromium ion with the copper wall of the vessel proposed by Gregory and Riddiford [72]. The determined diffusion transfer coefficient can be inserted in equation (3) to determine the rate of corrosion of the wall of the vessel. Moreover, diffusion controlled catalytic reactions taking place on a solid catalyst supported on the vessel wall can also benefit from the determined rate of mass transfer. The effects of the addition of drag reducing polymers or solid suspended particles on the rate of mass transfer/corrosion of the wall have also been studied.

2 Experimental Part

In this research, the rate of mass transfer controlled corrosion of the wall of an agitated vessel equipped with dual impeller is studied using the transport of the Cr^{6+} ion and subsequent reaction with the copper wall of the vessel [72] according to the equation:

$$3Cu + 7H_2SO_4 + K_2Cr_2O_7 \rightarrow 3CuSO_4 + Cr_2(SO_4)_3 + K_2SO_4 + 7H_2O$$

The rate of reaction is followed by titration of the solution against standard ferrous ammonium sulphate using diphenylamine indicator [73]. The agitated vessel (figure 1) consisted of cylindrical tank with pure copper wall and plexiglass bottom. The inside diameter of the tank was 12 cm

and its height was 26 cm. The tank had four baffles made of plexiglass with width of 1.2 cm and extending the whole height of the tank. The role of these baffles is to inhibit the formation of swirl flow of the liquid [1]. The agitation was carried by a dual- six flat blades Rushton disc turbine with diameter of 4 cm. This type of impellers produces radial flow in the solution.

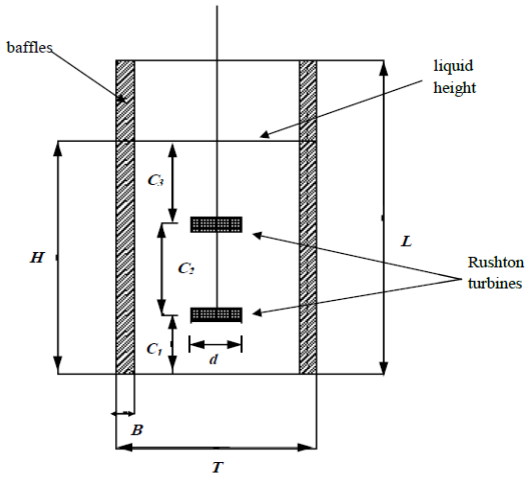

H	Liquid height	21 cm
L	Vessel height	26 cm
B	Baffle width	1.2 cm
T	Tank diameter	12 cm
d	Impeller diameter	4 cm
C_1	Lower impeller clearance from the bottom	4 cm
C_2	Impellers clearance	4, 8, and 11 cm

Figure 1: Schematic diagram and dimensions of the dual impeller agitated vessel.

Three different shafts with varying distance between the two impellers are used (4, 8 and 11 cm). The distance between the lower impeller and the bottom was kept constant at 4 cm. The shaft was rotated by means of electrical motor equipped with digital speed controller. The tank was filled with acidified dichromate solution up to the height of 21 cm. The solution composition was 0.003 M $K_2Cr_2O_7$ + x M H_2SO_4, where x is 0.5, 1, and 2. The physical properties of the solution are presented in table 1. Seven different rotation speeds were tested to study the rate of mass transfer (100- 700 rpm). Each tests lasted for 30 minutes and a sample was withdrawn every 5 minutes for titration. Temperature during test was 24 ±2 °C. A.R. grade chemicals and distilled water were used in the tests. The shaft and impellers were coated with epoxy to isolate them from the solution. Prior to each test, the wall surface was ground with fine abrasive paper and washed with distilled water.

Table 1: Physical properties of the solutions used.

	Density (gm/cm^3)	Viscosity (poise)	Diffusivity of Cr *10^6 (cm^2/s)	Sc Number
0.003 M $K_2Cr_2O_7$ and ½ M H_2SO_4				
0.003 M $K_2Cr_2O_7$ and 1 M H_2SO_4	1.06	1.035 *10^{-2}	9.55	1023
0.003 M $K_2Cr_2O_7$ and 2 M H_2SO_4	1.12	1.208 *10^{-2}	8.18	1322
0.003 M $K_2Cr_2O_7$ and 1 M H_2SO_4	1.02	9.273 *10^{-3}	10.7	850

Only the 8 cm-clearance dual impeller and the 0.5 M acidified dichromate were used in the polymer and suspended particles tests. The drag reducing polymer used was Polyox WSR 308, a product of DOW Chemicals. Three different concentrations of the polymer were used: 100, 200 and 400 ppm at five different agitation speeds (500, 700, 900, 1100 and 1300 rpm). For the suspended particles tests; Ceramic particles were ground and sieved to three different sizes: 150±25, 300±50 and 600±100 µm. Two different concentrations of particles were used: 10 and 25 g/L. To ensure the complete fluidization of the particles, the testing speeds were raised to 700, 900, 1100 and 1300 rpm. The increased rate of mass transfer at the presence of the ceramic particles resulted in the decrease of the test duration and thus samples were withdrawn at shorter time intervals. Tests were carried to check the stability of the dichromate against the polymer or the ceramic particles and it was found that the dichromate concentration does not change.

3 Results and Discussion

3.1 Rate of mass transfer at the wall of dual impeller agitated vessel

The mass transfer coefficient can be obtained from the decay of the dichromate concentration with time according to the first order reaction equation:

$$-\frac{dC}{dt} = \frac{kAC}{Q} \qquad (4)$$

which upon integration yields the form:

$$ln\left(\frac{C_0}{C}\right) = \frac{kA}{Q}t \qquad (5)$$

The values of k are calculated from the slopes of the $\boldsymbol{ln\left(\frac{C_0}{C}\right)}$ vs time (figure2).

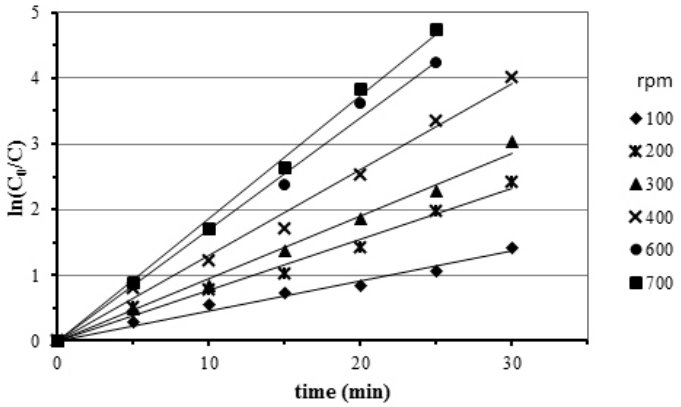

Figure 2: $ln(C_0/C)$ versus time curves for the 4 cm clearance between impellers at Sc=960.

Figures 3 and 4 revealed that the values of *K* increases with the increase of the clearance between the impellers and with the increase of the rotation speed.

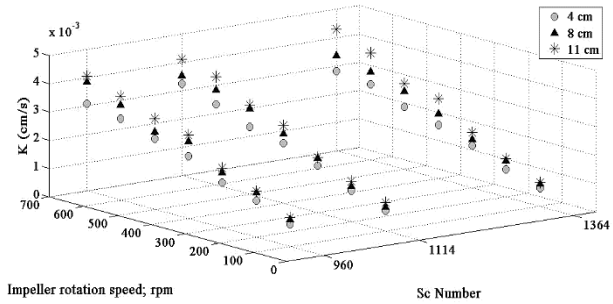

Figure 3: Values of mass transfer coefficient obtained at the different impellers spacing, different Schmidt numbers and different impeller rotation speed.

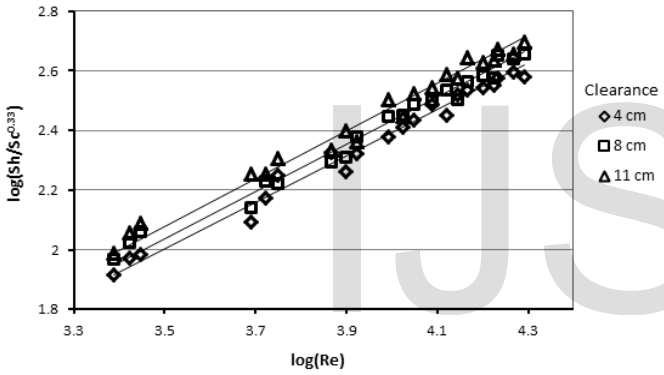

Figure 4: Effect of the impellers clearance on the rate of mass transfer.

The data are fitted by regression to yield the overall mass transfer correlation (figure 5):

$$Sh = 0.322\, Sc^{0.33} Re^{0.75} \left(\frac{c_2}{H}\right)^{0.185} \qquad (6)$$

which is valid for the conditions 960<*Sc*<13600, 2400<*Re*<19600 and 0.19< C_2/H <0.52. The mean percent relative error of this correlation is found to be 5 and the standard deviation is 4.1.

The increase of the mass transfer with the increase of the rotation speed is expected; the increase in the degree of turbulence will result in more eddies penetrating the diffusion sublayer attached to the wall and the increase of the amount of reactant available at the surface of reaction.

The increase in the mass transfer with the increase of the distance between the two impellers is due to decrease of volume of interaction between the two impellers; the two impellers become more independent of each other and little

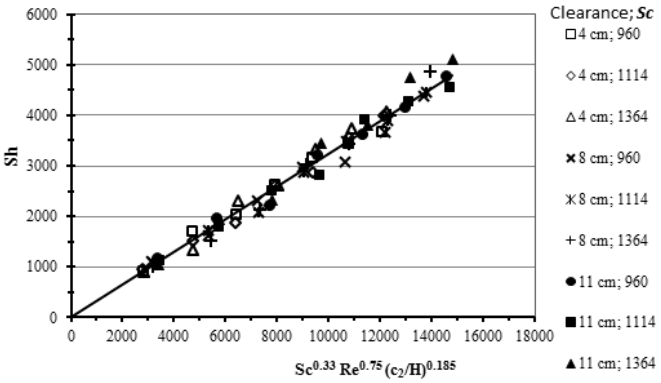

Figure 5: Mass transfer correlation for dual impeller agitated vessel.

interaction between the upper circulation loop of bottom impeller and lower circulation loop of upper impeller. This results in liquid at higher velocity and more eddies reaching larger area of the wall and a subsequent increase in the rate of mass transfer.

3.2 Comparison with single impeller

The mass transfer from the wall in a single impeller agitated vessel was determined by Askew and Beckmann [58] by the dissolution of benzoic acid technique. They presented their results for the vertical 6 blade Chemineer impeller in terms of the mass transfer correlation:

$$Sh = 3.30\, Sc^{0.3} Re^{0.55} \quad ; \quad 24000<Re<110000 \qquad (7)$$

For comparison, this correlation was used to estimate the values of mass transfer coefficient for a vessel of 12 cm internal diameter and 12 cm liquid height equipped with a 4 cm impeller and 4 baffles of 1.2 cm width. It has to be noted that both the Chemineer and Rushton turbine impellers produce radial flow. Figure 6 shows a comparison between the mass transfer coefficient at the wall of a single and a dual impeller agitated vessels. It is found that the coefficient of Reynolds Number is higher for the dual impeller (0.75 against 0.55). This might be a result of the low Reynolds Number used in this study (2400-19600 vs. 24000-110000). However, the values of the mass transfer coefficient are higher for the single impeller, and the difference decreases with the increase of the Reynolds Number (130% at 2800 and 57% at 20000).

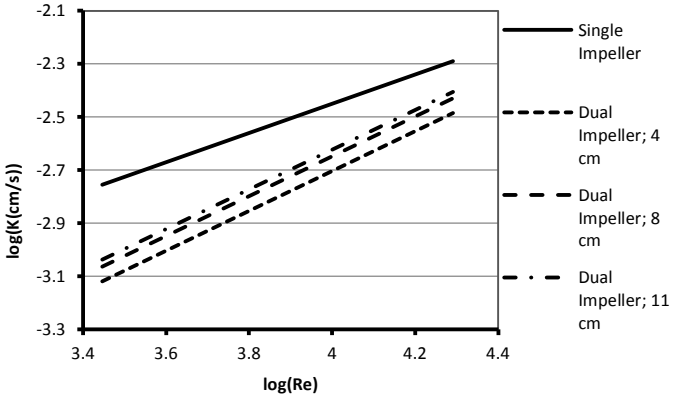

Figure 6: Values of estimated mass transfer coefficient for the single impeller (estimated from the work of Askew and Beckmann and the dual impeller with different spacing (current study) at Sc=960.

This can be the result of three reasons. The first reason is that the presence of the two impellers with two flow regimes poses impedance to the flow directed to the wall and decreasing the intensity of eddies reaching the wall compared to the single impeller system. The second reason is that Askew and Beckmann used the technique of the dissolution of benzoic acid wall which suffers from the development of surface roughness during the test and a change in the surface morphology, hydrodynamic conditions and surface area of the dissolving wall. The third reason is the difference of the values of *Re* and *Sc* numbers in the two studies.

3.3 Power consumption in mass transfer

Calderbank and Moo-Young [74] developed a relation between the mass transfer coefficient in agitated vessels to the power consumed as follows:

$$k = 0.13\left[\frac{\left(\frac{P}{Q}\right)\mu}{\rho^2}\right]^{1/4} Sc^{-2/3} \quad (8)$$

The power input in the process of agitation can be calculated according the equation [1], [75]:

$$P = N_P d^5 n^3 \rho \quad (9)$$

The power number, *Np*, is found in literature to be 4 for the case of 6 blade Chemineer single impeller [75] and 8.4, 10 and 10 for the case of dual impeller with clearance of 4, 8 and 11 cm respectively [7].

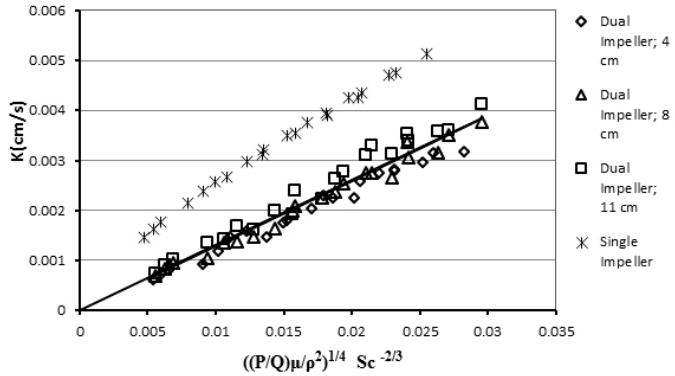

Figure 7: Comparison between the values of the mass transfer coefficient in terms of the specific power consumption.

Figure 7 shows a comparison of the values of mass transfer coefficient for single and dual impeller agitated vessel versus the calculated specific power consumption. The values estimated from the equation proposed by Calderbank and Moo-Young were superimposed on the figure.
It is noticed the good agreement between the experimental results for the dual impeller and the equation. This may suggest that the turbulence generated under the present conditions is isotropic turbulence for which Calderbank and Moo-Young equation was derived. On the other hand, the values for the single impeller are higher than expected. Again this can be a result from the different techniques used in the study and the developed roughness and attrition of the solid benzoic acid wall. Also it is probable that the turbulence generated by a single impeller is not isotropic as noticed by other investigators [76], [77]. It has to be mentioned that these results are in accordance with the reported finding that at equal power input, the dual impeller will have lower speed and lower shearing force [5].

3.4 Mass transfer at the different parts of the agitated vessel

Figure 8 compares the values of mass transfer coefficient at different parts of the agitated vessel. The values are estimated from the reported equations in literature (table 2). The results show that the maximum mass transfer occurs at the impeller itself, followed by the walls of the tank of the single impeller, followed by the baffles, the walls of dual impeller vessel and finally the flat bottom. This can be attributed to the difference of turbulence and eddies generated at these places, being highest near the impeller and lowest near the bottom and the wall. These findings point to which parts should be given more attention regarding corrosion protection when designing the agitated vessel parts.

Table 2: ***Mass transfer correlation for the different parts of the agitated vessels***

Agitated vessel part	Equation	Reynolds Number Range	Reference
Rushton Turbine	$Sh = 0.22\,Sc^{0.33}Re^{0.75}$	3350-37600	[32]

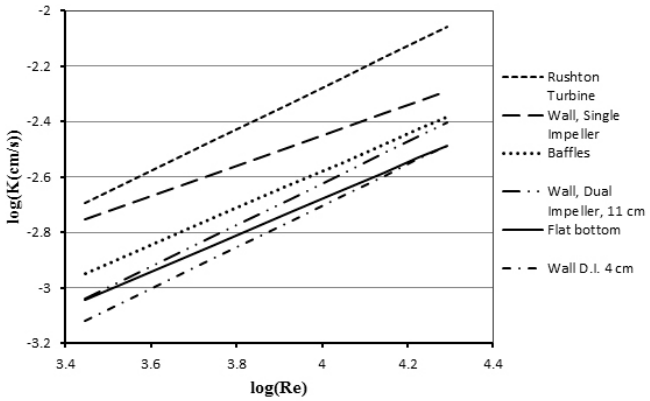

Figure 8: Mass transfer coefficient at different parts of the agitated vessel.

Wall/ Single Impeller	$Sh = 3.3\, Sc^{0.3} Re^{0.55}$ Vertical 6 blade Chemineer impeller	24000-110000	[58]
Wall/ Double Impeller	$Sh = 0.346\, Sc^{0.33} Re^{0.75} \left(\frac{C_2}{H}\right)^{0.185}$	2400-19600	
Baffles	$Sh = 0.336\, Sc^{0.33} Re^{0.67} Y^{-0.42}$ Y: dimensionless geometrical factor for the width of the baffle.	7500-60000	[53]
Flat Bottom	$Sh = 0.586\, Sc^{0.33} Re^{0.658}$ The impeller was 4 blade 45^{O} pitched turbine.	7330-61300	[28]

3.5 Effect of Drag Reducing Polymer

Figure 9 shows the effect of the addition of the drag reducing polymer to the solution while using the 8 cm dual impeller at Schmidt Number 960. The percent change in coefficient of mass transfer is calculated from:

$$Percent\ Change = \frac{|Value\ before - Value\ after|}{Value\ before} \quad (10)$$

The polymer addition resulted in a decrease in the value mass transfer coefficient. The mass transfer coefficient decreased with the increase of the polymer concentration and the decrease of the agitation speed: a maximum reduction of 35% occurred at 400 ppm polymer and 500 rpm. The results comply with the previous studies [28],[29],[30],[31],[32] that drag reducing polymers decrease the rate of mass transfer. Possible reason for this behaviour is the damping of strong vorticity fluctuation near the wall and small scale eddies in the hydrodynamic viscous sublayer. This will result in decrease of the disturbance of the diffusion sublayer and lower transport of the oxidizer to the wall. The increase in the reduction of mass transfer coefficient with the decrease of rotation speed is possibly due to the decrease in the rate of polymer degradation [35]. The results shows that drag reducing polymer can be used as corrosion inhibitor beside its main application in energy saving provided a continuous supply is secured for the make-up of the degraded polymer.

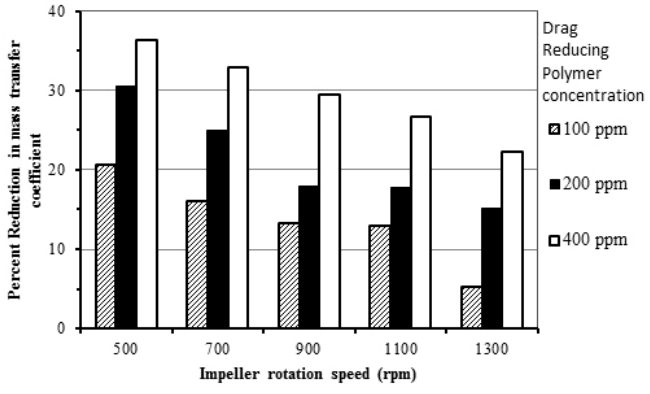

Figure 9: Effect of concentration of drag reducing polymer on the mass transfer coefficient.

3.6 Effect of suspended particles

Figure 10 shows the effect of the addition of ceramic particles. It is seen that the mass transfer coefficient increases with the increase of concentration of particles and with the increase of rotation speed. Generally, the increase of mass transfer coefficient is the result of collision and penetration of the solid particles with the diffusion sublayer formed at the wall. This results in disturbance at this layer and entrainment of fresh solution to the wall. These phenomena are associated directly with the number of particles and subsequently explain its increase with the decrease of the particle size and increase of particles concentration. Moreover, the higher momentum

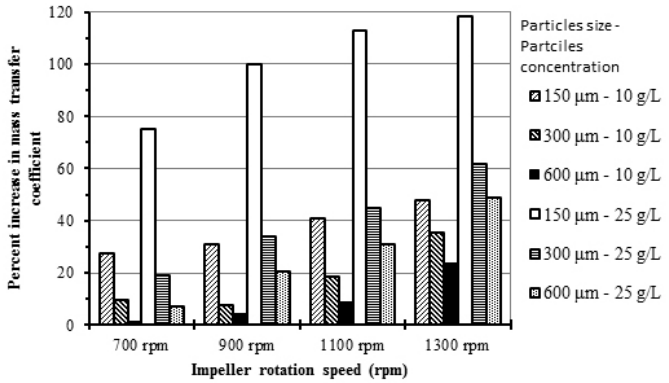

Figure 10: Effect of concentration and size of ceramic particles on the mass transfer coefficient.

gained by these particles at the higher rotational speeds results in more particles set in motion and higher number of collisions with the wall and at higher force. These results are consistent with previous studies [32], [38], [44], [78].

4 Conclusions

In this work, the mass transfer controlled corrosion of the wall of a dual impeller agitated vessel was studied. It was found that the rate of mass transfer increases with the increase of the clearance between the impellers and with the increase of agitation. A mass transfer correlation was formulated relating Sherwood Number to Schmidt Number, Reynolds Number and the dimensionless distance between the two impellers. Comparing the current results with previous studies showed that the mass transfer rate was lower than for the case of a single impeller. Moreover, the rate of corrosion will be lower than at the impeller but higher than the bottom of the vessel. Good agreement was obtained between the current results and the equation proposed by Calderbank and Moo-Young for the mass transfer per energy dissipated.

Furthermore, the addition of drag reducing polymer to the solution resulted in a decrease of the mass transfer; the higher decrease is obtained at the lower rotation speed and the higher polymer concentration. Thus, drag reducing polymer can be used as corrosion inhibitor provided of maintaining a constant supply to the vessel. On the other hand, the addition of suspended hard particles to the solution resulted in an increase in the rate of mass transfer; this increase depends on

the amount of particles and the impeller rotation speed. Therefore, the rate of corrosion is to be expected to increase if particles have to be present in the solution.

NOMENCLATURE

A	Area of mass transfer; cm^2
B	Baffle width
C	Concentration; mol/L
C_0	Initial concentration; mol/L
c_1	Lower impeller clearance from the bottom.
c_2	Distance between impellers.
c_3	Distance between top impeller and liquid line.
C_b	Concentration at wall
C_w	Concentration in bulk
CR	Corrosion rate; mm/year
d	Impeller diameter
D	Diffusion coefficient; cm^2/s
H	Liquid height
k	Mass transfer coefficient; cm/s
L	Vessel height
M	Molar
$M.Wt.$	Molecular Weight; g/mol
n	Rotation speed; rps
N	Mass flux; g/cm^2 s
Np	Power Number
P	Power; erg/s
Q	Volume of solution; cm^3
t	Time; s
T	Tank diameter
μ	Viscosity; g/cm s
ρ	Density; g/cm^3
Re	Reynolds Number $(\rho d^2 n/\mu)$
Sc	Schmidt Number $(\mu/\rho D)$
Sh	Sherwood Number (kH/D)

REFERENCES

[1] W.L. McCabe, J.C. Smith, and P. Harriott, *Unit Operations of Chemical Engineering*. Seventh ed. McGraw-Hill Chemical Engineering Series. 2005: McGraw-Hill

[2] H.A. Jakobsen, *Chemical Reactor modeling : Multiphase Reactive Flows*. 2008: Springer.

[3] J.R. Couper, W.R. Penney, J.R. Fair, S.M. Walas, R.C. James, W.R. Penney, R.F. James, and M.W. Stanley, *Mixing and Agitation*, in *Chemical Process Equipment (Second Edition)*. 2005, Gulf Professional Publishing: Burlington. p. 277-328.

[4] P.R. Gogate, A.A.C.M. Beenackers, and A.B. Pandit," Multiple-impeller systems with a special emphasis on bioreactors: a critical review". *Biochemical Engineering Journal*, 2000. **6**(2): p. 109-144.

[5] S.J. Arjunwadkar, K. Saravanan, A.B. Pandit, and P.R. Kulkarni," Optimizing the impeller combination for maximum hold-up with minimum power consumption". *Biochemical Engineering Journal*, 1998. **1**(1): p. 25-30.

[6] M. Nocentini, F. Magelli, G. Pasquali, and D. Fajner," A fluid-dynamic study of a gas—liquid, non-standard vessel stirred by multiple impellers". *The Chemical Engineering Journal*, 1988. **37**(1): p. 53-59.

[7] C. Pan, J. Min, X. Liu, and Z. Gao," Investigation of Fluid Flow in a Dual Rushton Impeller Stirred Tank Using Particle Image Velocimetry". *Chinese Journal of Chemical Engineering*, 2008. **16**(5): p. 693-699.

[8] A.R. Khopkar and P.A. Tanguy," CFD simulation of gas–liquid flows in stirred vessel equipped with dual rushton turbines: influence of parallel, merging and diverging flow configurations". *Chemical Engineering Science*, 2008. **63**(14): p. 3810-3820.

[9] V.R. Deshpande and V.V. Ranade," Simulation of flows in stirred vessels agitated by dual rushton impellers using computational snapshot approach". *Chemical Engineering Communications*, 2003. **190**(2): p. 236-253.

[10] I. Fořta, V. Machoňb, J. Hájekc, and E. Fialováb," Liquid circulation in a cylindrical baffled vessel of high height/diameter ratio with two impellers on the same shaft". *Collect. Czech. Chem. Commun.*, 1987. **52**: p. 2640-2653.

[11] G. Montante and F. Magelli," Liquid Homogenization Characteristics in Vessels Stirred with Multiple Rushton Turbines Mounted at Different Spacings: CFD Study and Comparison with Experimental Data". *Chemical Engineering Research and Design*, 2004. **82**(9): p. 1179-1187.

[12] G. Montante, K.C. Lee, A. Brucato, and M. Yianneskis," Numerical simulations of the dependency of flow pattern on impeller clearance in stirred vessels". *Chemical Engineering Science*, 2001. **56**(12): p. 3751-3770.

[13] S. Hiraoka, Y. Kato, Y. Tada, N. Ozaki, Y. Murakami, and Y.S. Lee," Power Consumption and Mixing Time in an Agitated Vessel with Double Impeller". *Chemical Engineering Research and Design*, 2001. **79**(8): p. 805-810.

[14] V. Hudcova, V. Machon, and A.W. Nienow," Gas–liquid dispersion with dual Rushton impellers". *Biotechnology and Bioengineering*, 1989. **34**(5): p. 617-628.

[15] G.R. Kasat, A.B. Pandit, and V.V. Ranade," CFD Simulation of Gas-Liquid Flows in a Reactor Stirred by Dual Rushton Turbines". *International Journal of Chemical Reactor Engineering*, 2008. **6**: p. A60.

[16] R. Zadghaffari, J.S. Moghaddas, and J. Revstedt," A mixing study in a double-Rushton stirred tank". *Computers & Chemical Engineering*, 2009. **33**(7): p. 1240-1246.

[17] S.U. Ahmed, P. Ranganathan, A. Pandey, and S. Sivaraman," Computational fluid dynamics modeling of gas dispersion in multi impeller bioreactor". *Journal of Bioscience and Bioengineering*, 2010. **109**(6): p. 588-597.

[18] X. Liu, Y. Bao, Z. Li, Z. Gao, and J.M. Smith," Particle Image Velocimetry Study of Turbulence Characteristics in a Vessel Agitated by a Dual Rushton Impeller". *Chinese Journal of Chemical Engineering*, 2008. **16**(5): p. 700-708.

[19] M. Al-Yaari, A. Soleimani, B. Abu-Sharkh, U. Al-Mubaiyedh, and A. Al-sarkhi," Effect of drag reducing polymers on oil–water flow in a

horizontal pipe". *International Journal of Multiphase Flow*, 2009. **35**(6): p. 516-524.

[20] A. Al-Sarkhi," Effect of mixing on frictional loss reduction by drag reducing polymer in annular horizontal two-phase flows". *International Journal of Multiphase Flow*, 2012. **39**(0): p. 186-192.

[21] T. Al-Wahaibi, Y. Al-Wahaibi, A. Al-Ajmi, N. Yusuf, A.R. Al-Hashmi, A.S. Olawale, and I.A. Mohammed," Experimental investigation on the performance of drag reducing polymers through two pipe diameters in horizontal oil–water flows". *Experimental Thermal and Fluid Science*, 2013. **50**(0): p. 139-146.

[22] C.M. White and M.G. Mungal," Mechanics and Prediction of Turbulent Drag Reduction with Polymer Additives". *Annual Review of Fluid Mechanics*, 2008. **40**(1): p. 235-256.

[23] P. Mavros, A. Ricard, C. Xuereb, and J. Bertrand," A study of the effect of drag-reducing surfactants on flow patterns in stirred vessels". *Chemical Engineering Research and Design*, 2011. **89**(1): p. 94-106.

[24] G. Montante, F. Laurenzi, A. Paglianti, and F. Magelli," A study on some effects of a drag-reducing agent on the performance of a stirred vessel". *Chemical Engineering Research and Design*, 2011. **89**(11): p. 2262-2267.

[25] R.S. Al-Ameeri,"Influence of drag reducing additives on power consumption in agitated vessels". *Chemical Engineering Communications*, 1987. **59**(1-6): p. 1-13.

[26] B.A. Toms. *Some observations on the flow of linear polymer solutions through straight tubes at large Reynolds numbers,*. in *Proceeding of the 1st International Congress on Rheology*. 1948. Amsterdam: North Holland Publication Company.

[27] Y. Kawaguchi, T. Segawa, Z. Feng, and P. Li," Experimental study on drag-reducing channel flow with surfactant additives—spatial structure of turbulence investigated by PIV system". *International Journal of Heat and Fluid Flow*, 2002. **23**(5): p. 700-709.

[28] Y.M. El-Shazly, R.R. Zahran, H.A. Farag, and G.H. Sedahmed," Mass transfer in relation to flow induced corrosion of the bottom of cylindrical agitated vessels". *Chem. Eng. Process.*, 2004. **43**(6): p. 745-751.

[29] G.H. Sedahmed, H.M. Asfour, M.M. Nassar, and O.A. Fadali," The effect of drag reducing polymers on the rate of mass transfer in electrochemical machining". *Corrosion Science*, 1982. **22**(8): p. 807-812.

[30] R.R. Zahran and G.H. Sedahmed," Galvanic corrosion of zinc in turbulently moving saline water containing drag reducing polymers". *Materials Letters*, 1997. **31**(1-2): p. 29-33.

[31] R.R. Zahran and G.H. Sedahmed," Effect of drag-reducing polymers on the rate of flow-induced corrosion of metals". *Materials Letters*, 1998. **35**(3-4): p. 207-213.

[32] G.H. Sedahmed, H.A. Farag, A.M. Kayar, and I.M. El-Nashar," Mass transfer at the impellers of agitated vessels in relation to their flow-induced corrosion". *Chemical Engineering Journal*, 1998. **71**(1): p. 57-65.

[33] Y. Wang, B. Yu, J.L. Zakin, and H. Shi," Review on Drag Reduction and Its Heat Transfer by Additives". *Advances in Mechanical Engineering*, 2011. **2011**: p. 17.

[34] T. Tsukahara and Y. Kawaguchi," Comparison of heat-transfer reduction in drag-reduced turbulent channel flows with different fluid and thermal boundary conditions". *Progress in Computational Fluid Dynamics, An International Journal*, 2011. **11**(3-4): p. 215-225.

[35] A.S. Pereira and E.J. Soares," Polymer degradation of dilute solutions in turbulent drag reducing flows in a cylindrical double gap rheometer device". *Journal of Non-Newtonian Fluid Mechanics*, 2012. **179–180**(0): p. 9-22.

[36] P. Menoud, L. Cavin, and A. Renken," Modelling of heavy metals adsorption to a chelating resin in a fluidized bed reactor". *Chemical Engineering and Processing: Process Intensification*, 1998. **37**(1): p. 89-101.

[37] N. Kuzmanić, R. Žanetić, and M. Akrap," Impact of floating suspended solids on the homogenisation of the liquid phase in dual-impeller agitated vessel". *Chemical Engineering and Processing: Process Intensification*, 2008. **47**(4): p. 663-669.

[38] Y. Zheng, Z. Yao, X. Wei, and W. Ke," The synergistic effect between erosion and corrosion in acidic slurry medium". *Wear*, 1995. **186–187, Part 2**(0): p. 555-561.

[39] P. Nova´k and A. Macenauer," Erosion-corrosion of passive metals by solid particles". *Corrosion Science*, 1993. **35**(1–4): p. 635-640.

[40] A. Neville, M. Reyes, and H. Xu," Examining corrosion effects and corrosion/erosion interactions on metallic materials in aqueous slurries". *Tribology International*, 2002. **35**(10): p. 643-650.

[41] H.M. Clark," Particle velocity and size effects in laboratory slurry erosion measurements OR… do you know what your particles are doing?". *Tribology International*, 2002. **35**(10): p. 617-624.

[42] C. Davis and P. Frawley," Modelling of erosion–corrosion in practical geometries". *Corrosion Science*, 2009. **51**(4): p. 769-775.

[43] J. Stojak and J. Talbot," Effect of particles on Polarization during Electrocodeposition using a Rotating Cylinder Electrode". *Journal of Applied Electrochemistry*, 2001. **31**(5): p. 559-564.

[44] R. Malka, S. Nešić, and D.A. Gulino," Erosion–corrosion and synergistic effects in disturbed liquid-particle flow". *Wear*, 2007. **262**(7–8): p. 791-799.

[45] B. Poulson," Complexities in predicting erosion corrosion". *Wear*, 1999. **233–235**(0): p. 497-504.

[46] K. Muroyama, T. Yoshikawa, S. Takakura, and Y. Yamanaka," Mass transfer from an immersed cylinder in three-phase systems with fine suspended particles". *Chemical Engineering Science*, 1997. **52**(21–22): p. 3861-3868.

[47] D. López, J.P. Congote, J.R. Cano, A. Toro, and A.P. Tschiptschin," Effect of particle velocity and impact angle on the corrosion–erosion of AISI 304 and AISI 420 stainless steels". *Wear*, 2005. **259**(1–6): p. 118-124.

[48] W. Bourgeois, J.E. Burgess, and R.M. Stuetz," On-line monitoring of wastewater quality: a review". *Journal of Chemical Technology & Biotechnology*, 2001. **76**(4): p. 337-348.

[49] M.G. Fontana, *Corrosion Engineering*. 1985, N.Y: McGraw-Hill.

[50] J.L. Dawson and C.C. Shih, *Corrosion under flowing conditions*, in *Flow Induced Corrosion: Proceedings of NACE*, K.J. Kennelly, et al., Editors. 1991: Houston, TX.

[51] B.K. Mahato, C.Y. Cha, and L.W. Shemilt," Unsteady state mass transfer coefficients controlling steel pipe corrosion under isothermal flow conditions". *Corrosion Science*, 1980. **20**(3): p. 421-441.

[52] A. Yabuki," Near-wall hydrodynamic effects related to flow-induced localized corrosion". *Materials and Corrosion*, 2009. **60**(7): p. 501-506.

[53] Y.M.S. El Shazly," Mass transfer controlled corrosion of baffles in agitated vessels". *Corrosion Engineering, Science and Technology*, 2011. **46**(6): p. 701-705.

[54] G.C. Shen, C.J. Geankoplis, and R.s. Brodkey," A note on particle--liquid mass transfer in a fluidized bed of small irregular-shaped benzoic acid particles". *Chemical Engineering Science*, 1985. **40**(9): p. 1797-1802.

[55] R.J. Goldstein and H.H. Cho," A review of mass transfer measurements using naphthalene sublimation". *Experimental Thermal and Fluid Science*, 1995. **10**(4): p. 416-434.

[56] A.K. Saroha," Solid–liquid mass transfer studies in trickle bed reactors". *Chemical Engineering Research and Design*, 2010. **88**(5–6): p. 744-747.

[57] M.H. Abdel-Aziz," Solid–liquid mass transfer in relation to diffusion controlled corrosion at the outer surface of helical coils immersed in agitated vessels". *Chemical Engineering Research and Design*, 2013. **91**(1): p. 43-50.

[58] W.S. Askew and R.B. Beckmann," Heat and Mass Transfer in an

Agitated Vessel". *Ind. Eng. Chem. Process Des. Dev.*, 1965. **4**(3): p. 311–318.

[59] J.A. Ruether, C.-S. Yang, and W. Hayduk," Particle Mass Transfer during Cocurrent Downward Gas-Liquid Flow in Packed Beds". *Industrial & Engineering Chemistry Process Design and Development*, 1980. **19**(1): p. 103-107.

[60] T. Yamagata, A. Ito, Y. Sato, and N. Fujisawa," Experimental and numerical studies on mass transfer characteristics behind an orifice in a circular pipe for application to pipe-wall thinning". *Experimental Thermal and Fluid Science*, (0).

[61] H. Mazhar, D. Ewing, J.S. Cotton, and C.Y. Ching," Experimental investigation of mass transfer in 90° pipe bends using a dissolvable wall technique". *International Journal of Heat and Mass Transfer*, 2013. **65**(0): p. 280-288.

[62] M.M. Zaki, I. Nirdosh, and G.H. Sedahmed," Mass transfer characteristics of reciprocating screen stack electrochemical reactor in relation to heavy metal removal from dilute solutions". *Chemical Engineering Journal*, 2007. **126**(2-3): p. 67-77.

[63] F.P. Berger and K.F.F.L. Hau," Mass transfer in turbulent pipe flow measured by the electrochemical method". *International Journal of Heat and Mass Transfer*, 1977. **20**(11): p. 1185-1194.

[64] Q.J.M. Slaimana and B.O. Hasan," Study on corrosion rate of carbon steel pipe under turbulent flow conditions". *The Canadian Journal of Chemical Engineering*, 2010. **88**(6): p. 1114-1120.

[65] O.N. Sara, J. Erkmen, S. Yapici, and M. Çopur," Electrochemical mass transfer between an impinging jet and a rotating disk in a confined system". *International Communications in Heat and Mass Transfer*, 2008. **35**(3): p. 289-298.

[66] N. Sonetaka, H.-J. Fan, S. Kobayashi, Y.-C. Su, and E. Furuya," Characterization of adsorption uptake curves for both intraparticle diffusion and liquid film mass transfer controlling systems". *Journal of Hazardous Materials*, 2009. **165**(1-3): p. 232-239.

[67] C.S. Tan and J.M. Smith," A dynamic method for liquid-particle mass transfer in trickle beds". *AIChE Journal*, 1982. **28**(2): p. 190-195.

[68] J. Wang and S.A. Shirazi," A CFD based correlation for mass transfer coefficient in elbows". *International Journal of Heat and Mass Transfer*, 2001. **44**(9): p. 1817-1822.

[69] J. Esteban Duran, F. Taghipour, and M. Mohseni," CFD modeling of mass transfer in annular reactors". *International Journal of Heat and Mass Transfer*, 2009. **52**(23-24): p. 5390-5401.

[70] S. Nesic, G. Adamopoulos, J. Postlethwaite, and D.J. Bergstrom," Modeling of turbulent-flow and mass-transfer with wall function and low Reynolds Number closures". *Canadian Journal of Chemical Engineering*, 1993. **71**(1): p. 28-34.

[71] G. Kear, S.-H. Huang, K. Bremhorst, and A. Purchase," Determination of diffusion controlled reaction rates at a solid/liquid interface using scanning electron microscopy". *Journal of Microscopy*, 2007. **226**(3): p. 218-229.

[72] D.P. Gregory and A.C. Riddiford," Dissolution of Copper in Sulfuric Acid Solutions". *J. Electrochem. Soc.*, 1960. **107**(12): p. 950-956.

[73] J. Mendham, R.C. Denney, J.D. Barnes, and M.J.K. Thomas, *Vogel's Quantitative Chemical Analysis*. 6 ed. 2000: Prentice Hall.

[74] P.H. Calderbank and M.B. Moo-Young," The continuous phase heat and mass-transfer properties of dispersions". *Chemical Engineering Science*, 1961. **16**(1-2): p. 39-54.

[75] G. Towler and R. Sinnot, *Chemical Engineering Design*. 2008: Elsevier.

[76] A.W. Nienow," Agitated vessel particle-liquid mass transfer: A comparison between theories and data". *The Chemical Engineering Journal*, 1975. **9**(2): p. 153-160.

[77] Y. Kawase and M. Moo-Young," Solid—turbulent fluid heat and mass transfer: A unified model based on the energy dissipation rate concept". *The Chemical Engineering Journal*, 1987. **36**(1): p. 31-40.

[78] C. Deslouis, A. Ezzidi, and B. Tribollet," Mass transfer enhancement by suspensions in a shear flow". *Journal of Applied Electrochemistry*, 1991. **21**(12): p. 1081-1086.